11th International Symposium on Magnetic Bearings
August 26-29, Nara, Japan

LEVITATION AND VIBRATION CONTROL OF A FLEXIBLE ROTOR BY USING ACTIVE MAGNETIC BEARING

Naoyuki Tanaka and Toru Watanabe
Watanabe Lab., Dept. of Mechanical Engineering, Science and Technology, Nihon Univ.
Chiyoda-ku, Tokyo 101-8308, JAPAN
E-mail:csna07020@g.nihon-u.ac.jp
Kazuto Seto
Seto Vibration Control Laboratory, Shinagawa, Tokyo, 140-0004, JAPAN
E-mail: seto@seto-vcl.com

ABSTRACT
This paper presents a new modeling method and a control system design procedure for a flexible rotor with many elastic modes by using active magnetic bearings. The purpose of our research is to rotate the rotor for passing through critical speeds caused by flexible modes. To achieve this, it is necessary to control motion and vibration of the flexible rotor simultaneously. The new modeling method named as Extended Reduced Order Physical Model is presented to express its motion and vibration uniformly. By using this model, a PID (Proportional-Integral-Derivative) controller to levitate the rotor and a LQ (Linear-Quadratic) controller to suppress its vibration are designed.

1. INTRODUCTION

Active magnetic bearings (AMB) systems have been applied to various machines such as grinding machines, vacuum pumps and energy storage flywheel system. Because AMB enables to support rotor without friction it is widely applied to high-speed rotors. However, as the rotation speed increases, more elastic modes of rotor and precession that is caused by gyroscopic effect appears. In this paper, a modeling technique for a flexible rotor-AMB system that can express vibration of elastic modes and gyroscopic effect is presented. Moreover, a control method applied to the model is also presented. The model is designed in order to describe an exact multi-degree-of-freedom dynamics of the flexible rotor-AMB system [1]. Utilizing the obtained model, we designed a feedback control system that combines both PID and LQ controllers. PID controller is used to levitate the rotor and stabilize the rigid modes of the rotor, whereas LQ control with state feedback loop is adapted to control many elastic modes of vibration. One of the authors had applied these modeling and control method to a flexible rotor [2]. We have been developing thinner, longer, heavier and more flexible rotor system. In this paper, the modelling and control method is applied to the rotor to evaluate their effectives.

2. CONTROL OBJECT AND ITS DYNAMIC CHARACTERISTICS

Figure 1 show the AMB device and a schematic diagram of the flexible rotor used as the control object in this research. Mass of this rotor weights about 10 kg. This rotor is levitated in thrust axis by using a PD (Proportional-Derivative) controller that is independently designed to LQ controller. And the coupling among thrust axis and other axes is ignored. Therefore, the main part of this research is to consider dynamics of the flexible rotor in radial direction.

Figure 2 shows the vibration mode shapes and their natural frequencies in free boundary condition obtained by using FEM. In this study, we aim to control rigid modes, 1st elastic mode, and 2nd elastic mode.

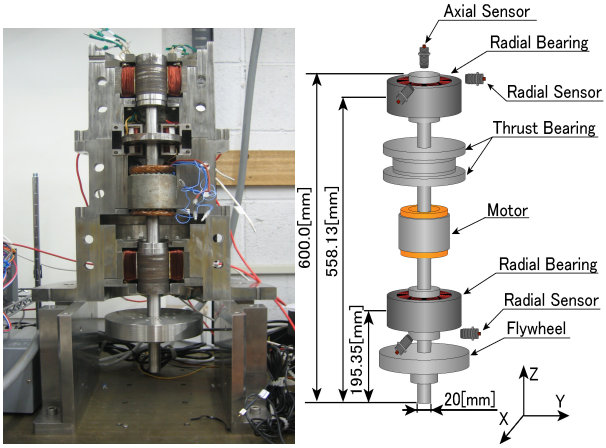

Fig.1 Flexible Rotor-AMB System

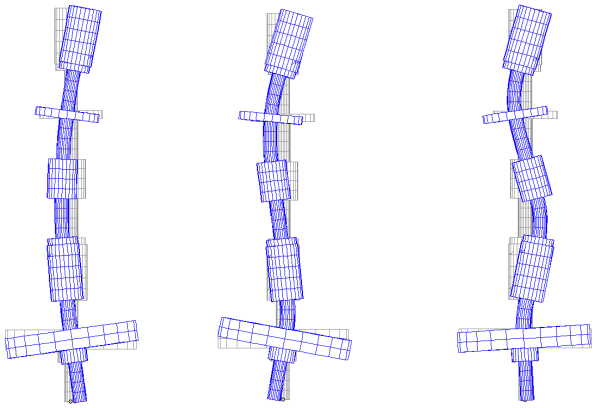

1st mode 163.7[Hz] | 2nd mode 391.4[Hz] | 3rd mode 691.6[Hz]

Fig.2 Modal Shapes Obtained by FEM

3. EXTENDED REDUCED ORDER PHYSICAL MODELING METHOD

3.1 Design Procedure of Extended Reduced Order Physical Model

In order to simulate and control flexible structures, authors have already developed an effective modelling method called "Extended Reduced Order Physical Modeling Method (EROM)" which can be treated in multi-body dynamics [3].

EROM is very useful for dynamic simulations and controller design of flexible structures because it is possible to treat three-dimensional non-linear systems and to express any distributed parameter system as a lumped parameter system. EROM can be applied not only to magnetic bearing, but also robotic arms, car bodies, etc. Using this method, good results have been obtained in our laboratory. Therefore, this model can be applied to wide range of fields.

In the model, flexible structure is composed of two kinds of rigid bodies and springs. One type of rigid body is named as "reference rigid body" that expresses motion, while the other type of rigid body named as "rigid bodies element" express vibration. The procedure of the extended reduced order physical modelling method is as follows,

1. Analyzes the mode shapes and identify the modal masses of each modes.
2. Choose the number of modes to be controlled and determine the positions of the rigid body elements.
3. Identify the mass matrix of the rigid body elements.
4. Identify the mass matrix of the reference rigid body.
5. Identify the stiffness matrix of the rigid body elements.
6. Construct the equations of motion.

In this study, the chosen mode number is determined to 4, two elastic modes to two directions(x, y axis direction). Then, number of the rigid body element is selected to 9. It is decided according to constraints on modal masses of rigid body element written as below.

1. Agreement of kinetic energy in each vibration mode.
2. Keep orthogonally to other vibration modes
3. Conservation of momentum in each vibration mode
4. Conservation of angular momentum in each vibration mode

Representing these constraints Matrix equation of constraints becomes written as below.

$$\begin{bmatrix} \boldsymbol{\Phi}_i^T \grave{\boldsymbol{\Phi}}_i \\ \boldsymbol{\Phi}_i^T \grave{\boldsymbol{\Phi}}_j \\ \boldsymbol{\Phi}^T \mathbf{I}_R \grave{\mathbf{I}}_X \\ \boldsymbol{\Phi}^T \mathbf{I}_R \grave{\mathbf{I}}_Y \\ \boldsymbol{\Phi}^T \mathbf{I}_R \grave{\mathbf{I}}_Z \\ \left(\grave{\mathbf{I}}_X^T \tilde{\mathbf{r}}_{Gm} \boldsymbol{\Phi}\right)^T \mathbf{I}_R + \boldsymbol{\Phi}^T \mathbf{I}_\Theta \grave{\mathbf{I}}_X \\ \left(\grave{\mathbf{I}}_Y^T \tilde{\mathbf{r}}_{Gm} \boldsymbol{\Phi}\right)^T \mathbf{I}_R + \boldsymbol{\Phi}^T \mathbf{I}_\Theta \grave{\mathbf{I}}_Y \\ \left(\grave{\mathbf{I}}_Z^T \tilde{\mathbf{r}}_{Gm} \boldsymbol{\Phi}\right)^T \mathbf{I}_R + \boldsymbol{\Phi}^T \mathbf{I}_\Theta \grave{\mathbf{I}}_Z \end{bmatrix} \begin{bmatrix} \boldsymbol{\xi} & \mathbf{0}_{3n\times 3n} \\ \mathbf{0}_{3n\times 3n} & \mathbf{I}_{3n\times 3n} \end{bmatrix} \begin{bmatrix} \mathbf{M}_{OB} \\ \mathbf{J}'_B \end{bmatrix} = \begin{bmatrix} \boldsymbol{\mu}_i \\ \mathbf{0} \\ \mathbf{0} \\ \mathbf{0} \\ \mathbf{0} \\ \mathbf{0} \\ \mathbf{0} \\ \mathbf{0} \end{bmatrix} \tag{1}$$

Where,

$$\mathbf{M}_{OB} = \begin{bmatrix} \mathbf{M}_{OB1} \\ \vdots \\ \mathbf{M}_{OBm} \end{bmatrix}, \quad \mathbf{J}'_B = \begin{bmatrix} \mathbf{J}'_{B1} \\ \vdots \\ \mathbf{J}'_{Bm} \end{bmatrix}$$

$$\boldsymbol{\xi} = diag\left[\mathbf{I}_{31} \quad \cdots \quad \mathbf{I}_{31}\right], \quad \mathbf{I}_{31} = \left[1 \quad 1 \quad 1\right]^T$$

$\boldsymbol{\Phi}$: Modal matrix obtained by vibration mode shapes

$\mathbf{M}_{OB}$: Mass matrix of rigid body elements

$\mathbf{J}'_B$: Moment of inertia matrix of rigid body elements

n : Number of reference modes

The mass matrix of the reference rigid body $\mathbf{M}_{OA}$ and the moment of inertia matrix $\mathbf{J}'_A$ are calculated to be equal to real mass $\mathbf{M}_{real}$ and real moment of inertia $\mathbf{J}'_{real}$ of the system in total. This is the reason why the model can express motion and vibration simultaneously.

$$\mathbf{M}_{OA} = \mathbf{M}_{real} - \boldsymbol{\eta}_m^T \mathbf{M}_{OB} \boldsymbol{\eta}_m \tag{2}$$

$$\mathbf{J}'_A = \mathbf{J}'_{real} - \left(\boldsymbol{\eta}_m^T \mathbf{J}' \boldsymbol{\eta}_m + \boldsymbol{\eta}_m^T \tilde{\mathbf{r}}_{Gm}^T \mathbf{M}_{OB} \tilde{\mathbf{r}}_{Gm} \boldsymbol{\eta}_m\right) \tag{3}$$

$$\boldsymbol{\eta}_m = \left[\mathbf{I} \quad \cdots \quad \mathbf{I}\right]^T \ (m\times 3)$$

The stiffness matrix $\mathbf{k}$ is obtained by the following equation.

$$\mathbf{k} = \mathbf{\Phi}^{-T}\boldsymbol{\omega}^2\boldsymbol{\mu}\mathbf{\Phi}^{-1} \quad (4)$$

Where $\boldsymbol{\omega}$ denotes a matrix including natural frequency of each modes.

Compared with modal masses of rigid body element that is a part of expressing vibration modes, mass of reference rigid body is designed so that the total mass of the model possess the same value with real mass of structure. Figure 3 shows a model of our rotor obtained by applying the EROM concept.

Next, the relation between the model and real rotor is shown by using this figure. Rigid body labelled as A denotes reference rigid body. Rigid bodies labelled as B1~B9 denote rigid body elements. B2 and B6 are subjected to control force in the radial direction. B1 and B7 are chosen as the sensing points in the radial displacement. The center of gravity of the rotor is located on B6. B9 denotes the bottom of the rotor. Each rigid body has 6 degrees of freedom (6DOF). Each rigid body elements and reference rigid body are connected by springs each other. Parameters of the rigid body elements and the reference rigid body are determined by the procedure mentioned above. The identified parameters are shown in Table 1.

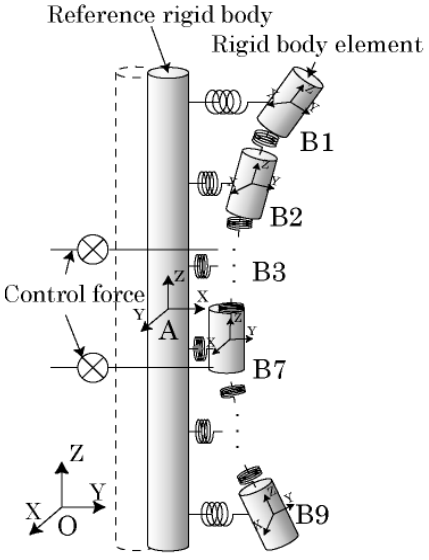

Fig. 3 Extended Reduced Order Physical Model

Table 1: Parameters of Rigid Body Elements and Reference Rigid Body

Element	Distance from center [mm]	Mass [kg]	Moment of Inertia [kgm2]	
			X-axis	Y-axis
B1	0.3767	0.00213	-0.06028	-0.06028
B2	0.3349	0.00678	0.061724	0.061724
B3	0.23721	0.01529	0.20591	0.20591
B4	0.1116	0.00346	0.098048	0.098048
B5	0	-0.0002	0.051546	0.051546
B6	-0.02791	0.00054	0.071626	0.071626
B7	-0.05581	0.00177	0.080004	0.080004
B8	-0.09767	0.00469	0.039069	0.039069
B9	-0.2233	0.00239	0.009597	0.009597
A	0	10.9777	-0.21497	-0.21497

3.2 Equations of Motion

In this section, we conduct equation of motion by using "the constraint addition method"[4]. First, the equations of motion of the reference rigid body A with no constraint are given like this.

$$\mathbf{M}_{OA}\dot{\mathbf{V}}_{OA} = \mathbf{F}_{OA} \quad (5)$$

$$\mathbf{J}'_A\boldsymbol{\Omega}'_{OA} + \tilde{\boldsymbol{\Omega}}'_{OA}\mathbf{J}'_A\boldsymbol{\Omega}'_{OA} = \mathbf{N}'_{OA} \quad (6)$$

$\dot{\mathbf{V}}_{OA}$: Velocity of reference rigid body,
$\mathbf{F}_{OA}$: External force on reference rigid body
$\boldsymbol{\Omega}'_{OA}$: Angular speed on reference rigid body,
$\mathbf{N}'_{OA}$: External torque on reference rigid body

Similarly, the equations of motion of the rigid body elements (B1~B9) without constraints are given like this

$$\mathbf{M}_{OB}\dot{\mathbf{V}}_{OB} = \mathbf{F}_{OB} \quad (7)$$

$$\mathbf{J}'_B\boldsymbol{\Omega}'_{OB} + \tilde{\boldsymbol{\Omega}}'_{OB}\mathbf{J}'_B\boldsymbol{\Omega}'_{OB} = \mathbf{N}'_{OB} \quad (8)$$

Each symbols denote same means in (7) and (8). Suffix "B" means the value of rigid body element B1~B9.Equations (5) ~ (8) denote equations of motion of the rotor without restraint. The generalized velocity H without constraints is given by

$$\mathbf{H} = \begin{bmatrix} \mathbf{V}_{OA} \\ \boldsymbol{\Omega}'_{OA} \\ \mathbf{V}_{OB} \\ \boldsymbol{\Omega}'_{OB} \end{bmatrix} \quad (9)$$

The mass matrix include the moment of inertia $\mathbf{M}^H$ and external force matrix $\mathbf{F}^H$ are given by

$$\mathbf{M}^H = \begin{bmatrix} \mathbf{M}_{OA} & 0 & 0 & 0 \\ 0 & \mathbf{J}'_A & 0 & 0 \\ 0 & 0 & \mathbf{M}_{OB} & 0 \\ 0 & 0 & 0 & \mathbf{J}'_B \end{bmatrix} \tag{10}$$

$$\mathbf{F}^H = \begin{bmatrix} \mathbf{F}_{OA} \\ \mathbf{N}'_{OA} \\ \mathbf{F}_{OB} \\ \mathbf{N}'_{OB} \end{bmatrix} \tag{11}$$

Equations (9) ~ (11) can also be written as

$$\mathbf{M}^H \dot{\mathbf{H}} = \mathbf{F}^H \tag{12}$$

Second, when $\mathbf{h}$ represents the modal velocity, the equation of motion with constraints will be derived. The generalized velocity $\mathbf{S}$ in the system with constraints is given by

$$\mathbf{S} = \begin{bmatrix} \mathbf{V}_{OA} \\ \mathbf{\Omega}'_{OA} \\ \mathbf{h} \end{bmatrix} \tag{13}$$

By using the constraint addition method[4], the equation of motion of the rigid body model is derived. The derived equations of motions by using the constraint addition method are as follows.

$$\mathbf{M}^S \dot{\mathbf{S}} = \mathbf{F}^S \tag{14}$$

$$\mathbf{H} = \mathbf{H}_S \mathbf{S} + \mathbf{H}_{\bar{S}} \tag{15}$$

$$\mathbf{M}^S = \mathbf{H}_S^T \mathbf{M}^H \mathbf{H}_S \tag{16}$$

$$\mathbf{F}^S = \mathbf{H}_S^T \left\{ \mathbf{F}^H - \mathbf{M}^H \left(\frac{d\mathbf{H}_S}{dt} \mathbf{S} + \frac{d\mathbf{H}_{\bar{S}}}{dt} \right) \right\} \tag{17}$$

Where,

$\mathbf{M}^S$: Generalized mass matrix constraints matrix
$\mathbf{F}^S$: Generalized force vector constraints matrix
$\mathbf{M}^H$: Unconstraint mass matrix
$\mathbf{H}$: Unconstraint generalized velocity
$\mathbf{F}^H$: Unconstraint force vector

3.3 State Space Representation

The equation of motion derived in the foregoing section is non-linear. In order to design the linear control system, it is necessary to linearize the equation of motion and to create a linearized state space model. Linearized equation (14) can be written as follows.

$$\mathbf{M}_0^S \delta \dot{\mathbf{S}} = \delta \mathbf{F}^S \tag{18}$$

Where the matrix with subscript 0 denotes linearized matrix around the equilibrium position. The relationship between generalized velocity $\mathbf{S}$ and generalized coordinate $\dot{\mathbf{Q}}$ with a derivative with respect to time is

$$\dot{\mathbf{Q}} = \mathbf{LS} \tag{19}$$

Equation (14) and (19) can be expressed in matrix form as

$$\frac{d}{dt}\begin{bmatrix} \mathbf{S} \\ \mathbf{Q} \end{bmatrix} = \begin{bmatrix} \left(\mathbf{M}^S\right)^{-1} \mathbf{F}^S \\ \mathbf{LS} \end{bmatrix} \tag{20}$$

This matrix equation is a first-order ordinary differential equation. From the above equation, the state-space form can be obtained as follows.

$$\dot{\mathbf{X}}_c = \mathbf{A}_c \mathbf{X}_c + \mathbf{B}_c \mathbf{U} \tag{21}$$

$$\mathbf{Y}_c = \mathbf{C}_c \mathbf{X}_c \tag{22}$$

When state valuable $\mathbf{X}_c$ is

$$\mathbf{X}_c = \begin{bmatrix} \mathbf{S} \\ \mathbf{Q} \end{bmatrix} \tag{23}$$

System matrix $\mathbf{A}_c$ can be derived as the partial derivative of the right hand side of Eq. (20) with respect to state valuable $\mathbf{X}_c$ [5]

$$\mathbf{A}_c = \frac{\partial}{\partial \mathbf{X}} \begin{bmatrix} \left(\mathbf{M}^S\right)^{-1} \mathbf{F}^S \\ \mathbf{S} \end{bmatrix} \Bigg|_{\substack{\mathbf{Q}=\mathbf{Q}_{eq} \\ \mathbf{S}=\mathbf{S}_{eq}}} \tag{24}$$

Also, the control matrix $\mathbf{B}_c$ can be derived as the partial derivative of the right hand side of Eq.(20) with respect to input $\mathbf{U}$.

$$\mathbf{B}_c = \frac{\partial}{\partial \mathbf{U}} \begin{bmatrix} \left(\mathbf{M}^S\right)^{-1} \mathbf{F}^S \\ \mathbf{S} \end{bmatrix} \Bigg|_{\substack{\mathbf{Q}=\mathbf{Q}_{eq} \\ \mathbf{S}=\mathbf{S}_{eq}}} \tag{25}$$

$$\mathbf{C}_c = \frac{\partial}{\partial \mathbf{X}} \begin{bmatrix} \mathbf{R}_{OB2} \\ \mathbf{R}_{OB7} \end{bmatrix} \Bigg|_{\substack{\mathbf{Q}=\mathbf{Q}_{eq} \\ \mathbf{S}=\mathbf{S}_{eq}}} \tag{26}$$

$\mathbf{Q}_{eq}$ and $\mathbf{S}_{eq}$ are the equilibrium positions of generalized coordinates and generalized velocitys, respectively.

4. NUMERICAL ANALYSIS OF ROTOR DYNAMICS

4.1 Frequency Response

Simulated frequency responses are shown in Fig.4 and 5. The resonance peaks appeared around 35Hz and 85Hz are of two rigid modes (parallel mode and conical mode), besides the peaks around 160Hz and 390Hz are 1st and 2nd elastic modes respectively. The gyroscopic effect is clearly appeared in Fig.5 though it did not appear in Fig.4. Figure 5 shows frequency response of the model with rotational speed at 30 Hz. It is recognized that the gyroscopic effect act to split the natural frequency of each mode into two natural frequencies.

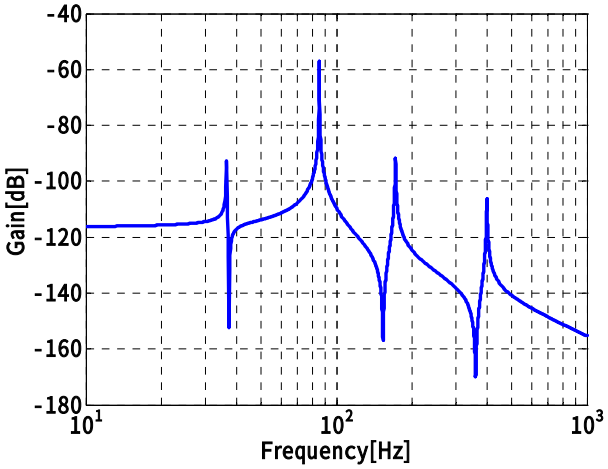

Fig.4 Frequency Response of the Model at Rotational Speed 0[Hz]

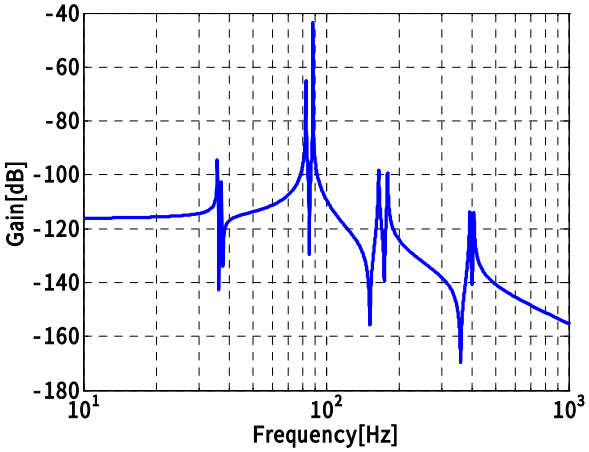

Fig.5 Frequency Response of the Model at Rotational Speed 30[Hz]

4.2 Campbell Diagram

In order to demonstrate the usefulness of extended reduced order physical model that can treat the gyroscopic effect of the flexible rotor, variation of natural frequencies depending on rotational speed is examined by calculation. Figure 6 shows the relationship between rotational speed and natural frequency of the rotor used in this study. Natural frequencies of two elastic modes located at 160 Hz and 390 Hz under 0 rpm are split into two frequencies as the rotational speed increases.

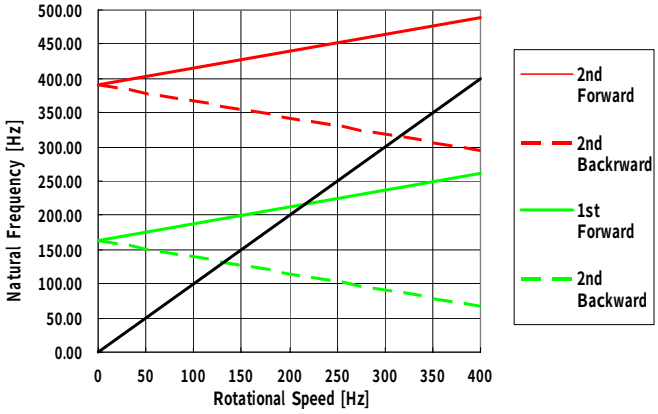

Fig.6 Campbell Diagram

5. CONTORL SYSTEM DESIGN

5.1 PID Control

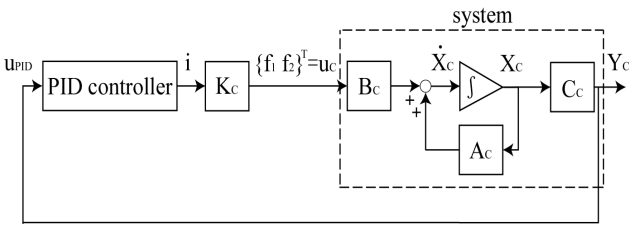

Fig.7 Block Diagram

Since the rotor-AMB system is essentially unstable and can not be levitated without control, PID control is used to stabilize the system. The two rigid modes (parallel and conical) are also controlled. Figure 7 shows the associated block diagram.

The transfer function of PID controller is designed as follows,

$$\frac{i}{u_{PID}} = \left(\frac{\alpha_1 T_{d1} s + 1}{T_{d1} s + 1}\right)\left(\frac{\alpha_2 T_{d2} s + 1}{T_{d2} s + 1}\right) \tag{27}$$

It can be written in the state space representation as below,

$$\dot{\mathbf{X}}_h = \mathbf{A}_h \mathbf{X}_h + \mathbf{B}_h u_h \tag{28}$$

$$Y_h = \mathbf{C}_h \mathbf{X}_h + D_h u_h \tag{29}$$

Where,

$$\mathbf{X}_h = \begin{bmatrix} \dot{e} \\ e \end{bmatrix}, \quad u_h = u_{PID}, \quad Y = i$$

$$\mathbf{A}_h = \begin{bmatrix} -\dfrac{(T_{d1} + T_{d2})}{T_{d1} T_{d2}} & -\dfrac{1}{T_{d1} T_{d2}} \\ 1 & 0 \end{bmatrix}$$

$$\mathbf{B}_h = \begin{bmatrix} 1 \\ \hline T_{d1}T_{d2} \\ 0 \end{bmatrix}$$

$$\mathbf{C}_h = \begin{bmatrix} \alpha_1 T_{d1} + \alpha_2 T_{d2} & 1 \end{bmatrix}$$

$$D_h = \alpha_1 \alpha_2$$

The parameter and frequency response of the designed PID controller are shown as follows.

$$\alpha_1 = 5.77511299392671$$
$$\alpha_2 = 3.22442479388603$$
$$T_{d1} = 8e-003$$
$$T_{d2} = 8e-003$$

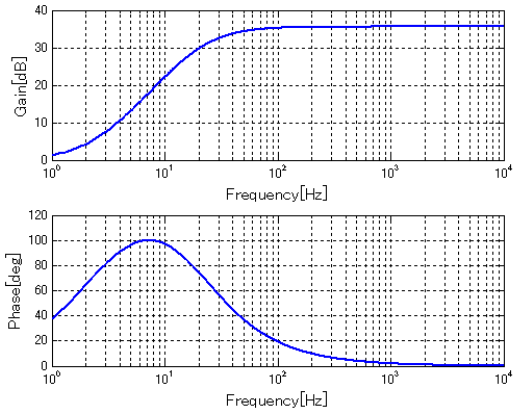

Fig.8 Frequency Response of PID Controller

5.2 Filtered LQ Control Combined with PID

Figure 9 shows a block diagram of the system combined PID controller with LQ controller. The feedback gain vectors, $\mathbf{K}_{PID}$ is tuning and $\mathbf{K}_{LQ}$ is obtained by applying LQ control law to the augmented system.

Derived non-linear equation (14) is linearized to obtain state equation. The state equation and output equation combined with PID control system are shown as follows.

$$\dot{\mathbf{X}} = \mathbf{AX} + \mathbf{BU} \tag{30}$$

$$\mathbf{Y} = \mathbf{CX} \tag{31}$$

Here,

$$\mathbf{A} = \begin{bmatrix} \mathbf{A}_f & \mathbf{0}_{8\times12} & \mathbf{0}_{8\times16} \\ \mathbf{B}_h\mathbf{C}_f & \mathbf{A}_h & \mathbf{0}_{12\times16} \\ \mathbf{0}_{16\times8} & \mathbf{B}_s\mathbf{C}_h & \mathbf{A}_s \end{bmatrix}$$

$$\mathbf{B} = \begin{bmatrix} \mathbf{B}_f \\ \mathbf{0}_{12\times14} \\ \mathbf{0}_{16\times4} \end{bmatrix}$$

$$\mathbf{C} = \begin{bmatrix} \mathbf{0}_{4\times8} & \mathbf{0}_{4\times12} & \mathbf{C}_s \end{bmatrix}$$

$$\mathbf{X} = \begin{bmatrix} \mathbf{X}_f \\ \mathbf{X}_h \\ \mathbf{X}_c \end{bmatrix}$$

$$\mathbf{U} = -\left(\mathbf{I}_{4\times4}\mathbf{C} + \mathbf{K}\right)\mathbf{X}$$

Where, the state variable is defined as follows.

$$\mathbf{X}_f = \begin{Bmatrix} \dot{x}_{f1} & x_{f1} & \dot{y}_{f1} & y_{f1} & \dot{x}_{f2} & x_{f2} & \dot{y}_{f2} & y_{f2} \end{Bmatrix}^T$$

$$\mathbf{X}_h = \begin{Bmatrix} \ddot{e}_{x1} & \dot{e}_{x1} & e_{x1} & \ddot{e}_{y1} & \dot{e}_{y1} & e_{y1} \\ \ddot{e}_{x2} & \dot{e}_{x2} & e_{x2} & \ddot{e}_{y2} & \dot{e}_{y2} & e_{y2} \end{Bmatrix}^T$$

$$\mathbf{K} = \begin{bmatrix} \mathbf{K}_f & \mathbf{K}_{lq} \end{bmatrix}$$

Thus, the state equation of the augment system is written as follows.

$$\dot{\mathbf{X}}_c = \mathbf{A}_c\mathbf{X}_c + \mathbf{B}_c\mathbf{U}_c \tag{32}$$

$$\mathbf{Y}_c = \mathbf{C}_c\mathbf{X}_c \tag{33}$$

Here,

$$\mathbf{A}_c = \begin{bmatrix} \mathbf{A}_H & \mathbf{0} \\ \mathbf{B}_S & \mathbf{A}_S \end{bmatrix}$$

$$\mathbf{B}_c = \begin{bmatrix} \mathbf{B}_H & \mathbf{0} \end{bmatrix}$$

$$\mathbf{C}_c = \begin{bmatrix} \mathbf{0} & \mathbf{C}_S \end{bmatrix}$$

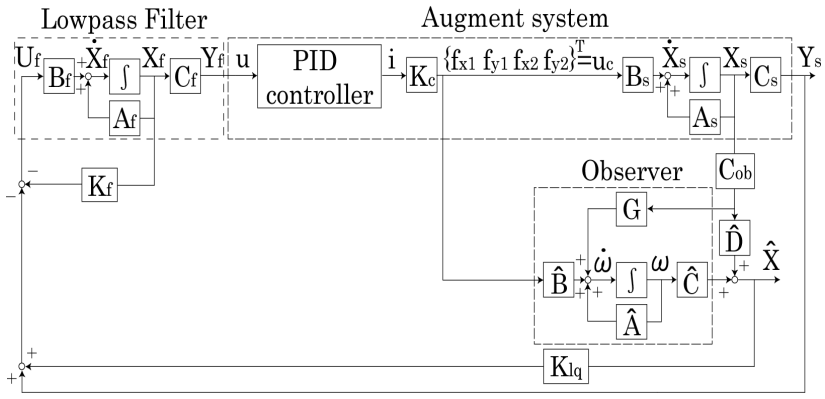

Fig.9 Block Diagram of Augmented System

6. COMPUTER SIMULATION

In this chapter, simulation results by using only PID controller or controller combining PID with LQ are shown in Fig.10, 11 and 12. These frequency responses are calculated in case that the rotor is at critical speeds obtained by Fig.6, the external disturbance is input on rigid body element B2 and displacement output is observed at B1. It is clearly shown that the rigid modes are well suppressed when only PID controller is used, while, the elastic modes are not suppressed. This is because PID controller is used merely for controlling the rigid modes in this study. Whereas, the controller combined PID with LQ is acted well to control the 1st and 2nd elastic modes. Especially, split two natural frequencies caused by gyroscopic effect are well controlled. The robustness of state feedback control realized such effect.

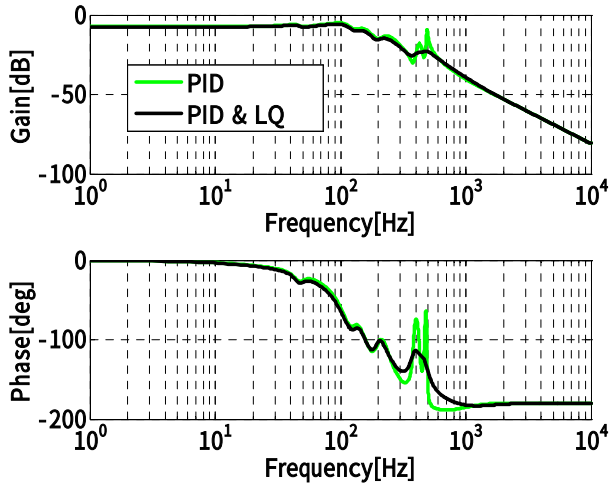

Fig.10 Simulation Results of Frequency Response at 130(Hz)

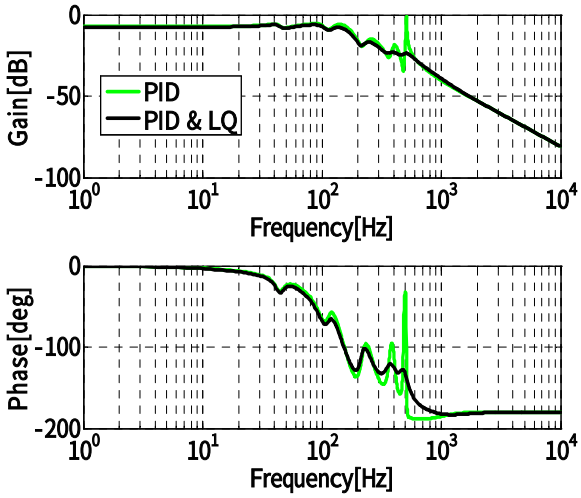

Fig.11 Simulation Results of Frequency Response at 210(Hz)

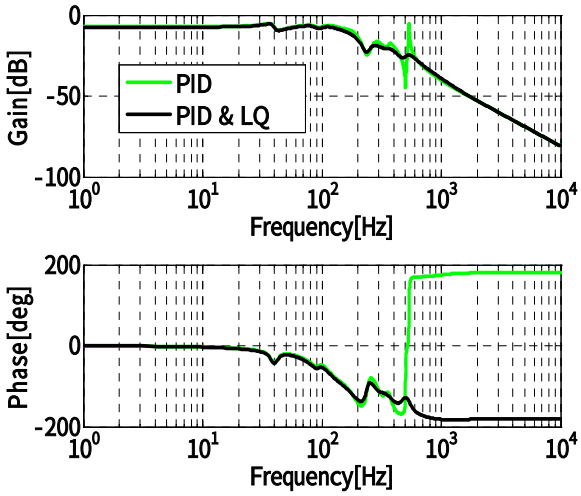

Fig.12 Simulation Results of Frequency Response at 320(Hz)

7. EXPERIMENTAL RESULTS OF LEVITATION IN THE THRUST DIRECTION

In this paper, rotor is levitated in thrust axis by using a PD controller that is independently designed to LQ controller. And thrust AMB controller is independent with radial AMB controller. In this chapter, experimental results of levitation in the thrust direction by using PD controller are shown. Figure 13 shows a block diagram of thrust AMB system.

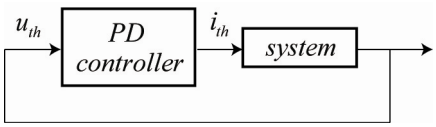

Fig. 13 Block Diagram of Thrust AMB System

The transfer function of PD controller is,

$$\frac{i_{th}}{u_{th}} = k_D s + k_P \qquad (34)$$

k_D : D-gain

k_P : P-gain

Experimental results of levitation in the thrust direction by using PD controller are shown in Fig.14 and Fig.15. Simulation results are also presented for comparison. The simulation model is one degree-of-freedom system. So the experimental and simulation results show a little difference. However, the basic characteristics agree well. We plan to design control system in a radial direction according to these results.

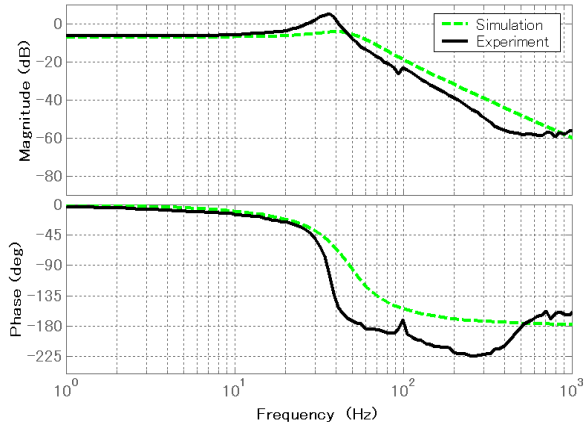

Fig. 14 Frequency Response of Thrust Direction by using PD controller

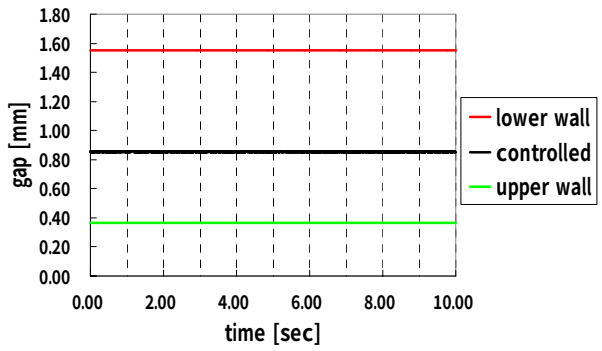

Fig. 15 Time History Response of Thrust Direction by using PD controller

8. CONCLUSIONS

In this paper, a controller design procedure for a flexible rotor-AMB system has been investigated. The proposed modeling technique named as Extended reduced order physical model was applied to obtain the multi- degree of freedom model of the flexible rotor-AMB system. A controller is designed by using controller combined PID with LQ control were introduced to stabilize the flexible rotor and to control flexible bending vibration. Computer simulations are carried out and the controller obtained by using the presented procedure achieved good control performance.

REFERENCES

[1] H. Ueyama, “Mechanics Control of Turbo Molecular Vacuum Pump with Active Magnetic Bearings,” JSME, Vol.103 Num.978, pp.330-330, 2000.

[2] K. Seto, et al, “A New Modeling Technique and Control System Design of Flexible Rotor Using Active Magnetic Bearings for Motion an Vibration Control,” Proc. of the 9th International Symposium on Magnetic Bearings, CD-ROM,2004.

[3] T. Sagane, H. Tajima, K. Seto, “Modeling and Control of Elastic Bodies: 1st Report, Proposals the Extended Reduced Order Physical Model,” JSME, Vol.68 Num.673, pp.2591-2598, 2002

[4] H.Tajima, “Proposals and Consideration on Derivation Methods of Equations of Motion,” Proc. of Dynamics & Design conference 2000, JSME, Tokyo, Japan, CD-ROM

[5] S. Yamamoto, T. Sagane , H. Tajima, K. Seto, “A New Modeling Method of Two-link Flexible Robot Arms,” Proc. of 10th Asia-Pacific vibration conference, pp.777-782, 2003